Hindawi
International Transactions on Electrical Energy Systems
Volume 2023, Article ID 3648488, 21 pages
https://doi.org/10.1155/2023/3648488

Review Article

A Comprehensive Review of Various Topologies and Control Techniques for DC-DC Converter-Based Lithium-Ion Battery Charge Equalization

G. Sugumaran and N. Amutha Prabha

School of Electrical Engineering, Vellore Institute of Technology, Vellore, India

Correspondence should be addressed to N. Amutha Prabha; amuthaprabha@vit.ac.in

Received 18 July 2022; Accepted 3 October 2022; Published 29 March 2023

Academic Editor: Ci Wei Gao

Worldwide, electric vehicle (EV) sales are booming nowadays due to the rapid increase in the cost of fossil fuels. Lithium-ion batteries are very familiar in the EV industry because of their high energy per unit mass relative to other electric energy storage systems. To obtain the required voltage, several lithium-ion batteries are connected serially. Due to manufacturing inconsistencies, the voltage of serially connected cells is not always equal, which might result in a charge imbalance. This imbalance may reduce the battery's life span due to the action of undercharging and overcharging. Battery charge equalisation (BCE) is challenging because it requires a constant voltage level in each cell. Various topologies and control strategies have been proposed in the past literature to build and improve the BCE. This study extracts the recently proposed DC-DC converter-based topologies for BCE. This study then gives a comparative analysis of various control strategies used in BCE and ends with implementing control strategies with BCE topology using a DC-DC converter. This study incorporates contextualised topologies used by BCE with design, operation, and applications. Extensive simulation results are provided to compare the performance of DC-DC converter-based BCE topologies in balancing speed. Also, a comprehensive comparison of various converter topologies and control strategies has been carried out for future investigation.

1. Introduction

The widespread usage of crude oil in internal combustion engine vehicles, such as gasoline, diesel oil, and liquefied petroleum gas, has significant effects like CO_2 emissions [1]. Furthermore, the global depletion of fossil resources and, as a result, rising crude oil costs pose a significant challenge to the vehicle industry. Electric vehicles (EVs) have already been widely adopted in the automotive industry as the most promising substitutes for decreasing CO_2 emissions and global warming concerns [2]. The most popular EVs, such as hybrid electric vehicles (HEVs), plug-in hybrid electric vehicles (PHEVs), and pure electric vehicles or battery electric vehicles (BEVs), have become popular options due to their ability to address the issues that fossil fuel vehicles pose.

According to a Bloomberg analysis, worldwide EV sales are increasing with time, with 64 million EVs expected to be delivered by 2050, accounting for half of all passenger car sales, as illustrated in Figure 1. Various electric sources power electric vehicles, but most researchers consider rechargeable batteries the finest.

The selection of batteries for electric vehicles is one of the most challenging tasks. Various batteries used in electric cars are listed in Table 1 with their merits and demerits. From the table, it can be seen the lithium-ion battery has plenty of prices compared to others. Even though it is more expensive, it is mainly recemented in EV industries. Currently, the manufacturing of lithium-ion batteries is increasing daily [3, 4]. The year-wise growth of lithium-ion battery manufacturing is depicted in Figure 2.

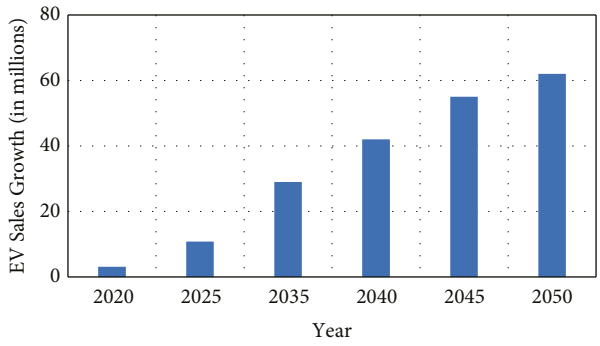

Figure 1: Global EV sales growth (2020–2050).

Table 1: Classification of batteries used in EV.

EV batteries	Advantages	Disadvantages
Lithium-ion	High charging capacity, long life span, compact size, high power density, and low self-discharge	More expensive
Nickel metal hydrate	High power density and long life span	High self-discharge, high temperature, and more expensive
Lead acid	Inexpensive, safe, reliable, and simple in production and recycling	Bulky and low specific energy
Solid state	Low temperature, high energy density, and long life span	Manufacturing is difficult
Aluminium ion	Fast charging, high capacity, safer to handle, low cost, and high energy density	Low voltage, low efficiency, and material corrosion

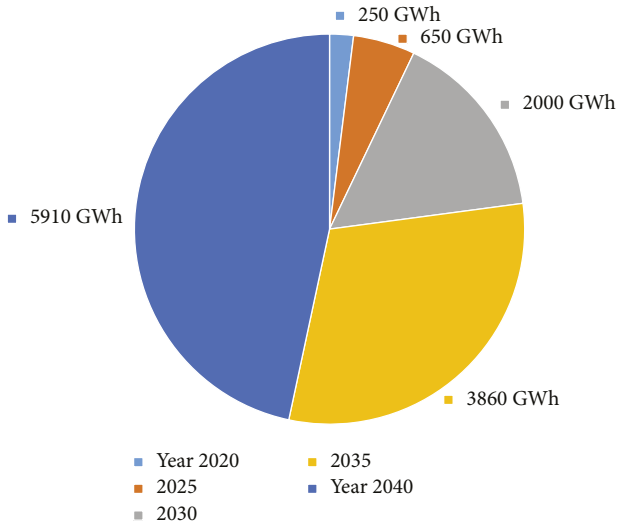

Figure 2: Development of global Li-ion batteries in GWh.

Following that battery selection, the choice of battery charging topology is also a critical task. Various battery charging topologies utilised in the current scenario are depicted in Table 2. Battery charging topologies with their power range, charger power, and charging time were estimated using this table. Two systems are utilised: alternating current (AC) and direct current (DC). According to the utility of assessing topology, again, it is classified into two types, namely, onboard charging (for low-power AC charging) and off-board charging (for high-power AC/DC charging) [5].

Battery charge equalisation is one of the most critical concerns in electric vehicles. Many studies have been conducted to improve and develop the BCE [6]. Numerous BCE topologies, as well as several control mechanisms for boosting BCE efficiency, were also anticipated in this paper. Following the introduction, Section 2 elaborates on the lithium-ion battery charge equalisation; under that, the causes of cell imbalance, the module of the BCE system, and different types of BCE will be discussed. The converter-based BCE is examined in Section 3. Under that, various energy flow techniques and DC-DC converter topologies are discussed. Section 4 covers the control strategies of BCE; classification of control variables and multiple methods of SOC estimation are included in this section. Section 5 elaborates on the analysis of dc-dc converter topologies, which was carried out using MATLAB simulation; the comparative chart of converter-based BCE topologies was included in this section, which covers several elements such as energy transfer technology, balancing time, size, cost, power loss, and efficiency. Finally, this article was concluded with a conclusion.

2. Lithium-Ion Battery Charge Equalisation

Battery charge equalisation is the most severe problem with electric vehicles. The EV's single battery is insufficient to keep it running. To make a battery pack, the "*N*" number of cells must be connected in parallel or series. This is dependent on the vehicle's capacity. Due to variations in internal resistance, all battery pack cells are not uniformly charged or drained. This could harm the battery pack as a whole. The cell in the battery pack that is overcharged or

Table 2: Various battery charging topologies for EV.

Charging topology	Power level	Power supply	Charger power (approx)	Charging time (approx for 24 kWh battery)
AC charging station	Level 1, residential	120/230 V and 12 A–16 A, single phase	1.4 kW–1.9 kW	17 hours
AC charging station	Level 2, commercial	208–240 V and 15 A-18 A, single/split phase	3.1 kw–19.2 kW	8 hours
DC charging station	Level 3, fast charging	300–600 V and max 40 A, poly phase	120–240 kW	30 minutes

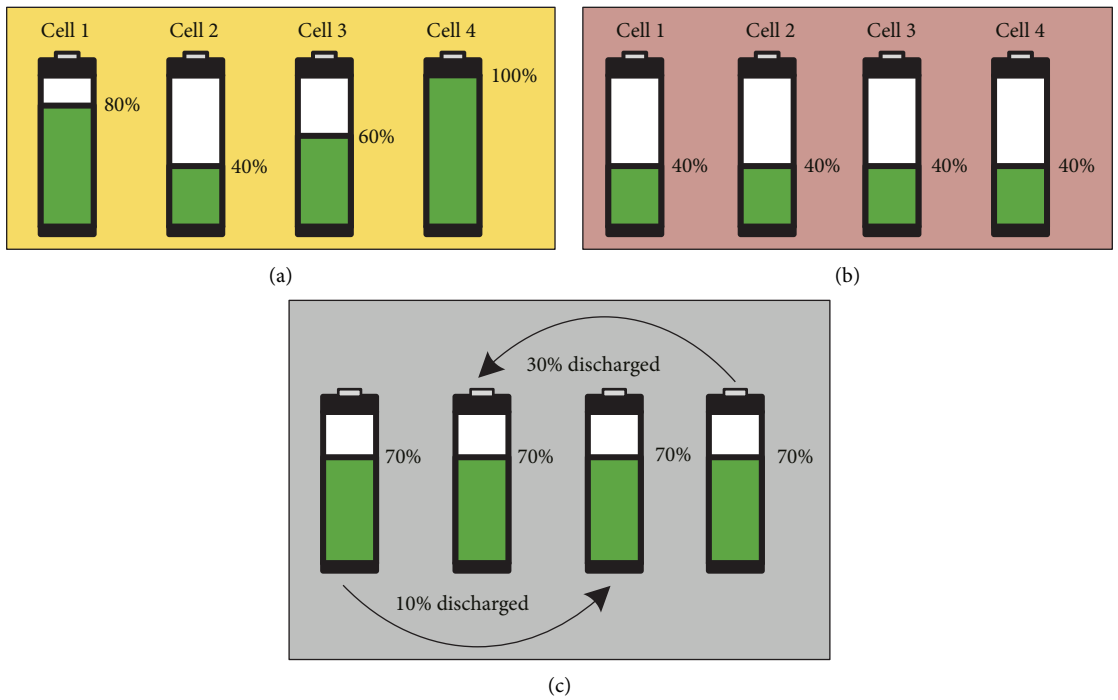

Figure 3: Battery charge equalisation methods. (a) Charge imbalance among cells. (b) Passive method of BCE. (c) Active method of BCE.

undercharged will explode or lose energy. This may cause significant harm to the overall battery pack and shorten the battery's lifespan [7, 8].

The charge imbalance among four cells is depicted in Figure 3(a). Cell 2 is undercharged, while cell four is overcharged, as determined by the state of charge (SOC). BCE approaches are utilised to provide a balanced voltage across all cells. The passive and active BCE methods are the most employed. Figure 3(b) shows the passive technique of BCE, in which a balanced voltage is maintained across all cells by dissipating excessive charges using resisters and carrying a 40% charge across each cell, but this may result in energy loss and heat concerns. The active technique of BCE is shown in Figure 3(c); here, the excessively charged cells are identified through the controller, and the excess energy is discharged to the undercharged cells, resulting in a balanced voltage among all cells and a 70% charge maintained without energy losses. The impact of battery charge equalisation on battery life span and reliability is as follows: battery balancing can maximise the capacity of the battery pack, it protects the battery from critical conditions like overcharging and over-discharging, and battery balancing is also used to maintain the battery environment at room temperature; it protects the battery from cell degradation [9, 10].

2.1. The Module of the Battery Charge Equalisation System. The fundamental block diagram for an EV with a battery charge equalisation system is shown in Figure 4. The battery charge equalisation is a part of the battery management system (BMS). BMS is the heart of EV. It consists of battery monitoring, charge equalisation, thermal management, power optimisation, and communication. The BMS monitors various battery data like the voltage, current, and temperature for analysing SOC, charging time, discharging time, and balancing time [11]. The BMS is connected between the battery pack and controller; the function of the BMS is as follows, BMS is primarily concerned with balancing the SOC and voltage of individual cells. BMS safeguards the battery against overcurrent, overvoltage, and undervoltage conditions. The BMS will continuously monitor the temperature of the battery pack and isolate it if the temperature is exceeded. BMS also monitors current, voltage, SOC, and SOH to ensure efficient charging and discharging [12, 13].

2.2. Classification of BCE Topologies. The numerous types of battery equalisation are depicted in Figure 5. The structure of battery equalisation is primarily divided into two types: passive and active [14, 15]. The passive method includes resister-based equalisation, whereas the active method includes an inductor, capacitor, and converter-based equalisation. This article emphasises the technique that is highlighted [16].

3. Converter-Based Battery Charge Equalisation

The battery charge equalisation will be accomplished in passive and active ways. The dynamic technique will outperform the passive method in terms of maximum power gain because excessive energy will be lost as heat energy in the passive mode. The most prevalent types of active charge equalisation include capacitance-based, inductance-based, transformer-based, and DC-DC converter-based charge equalisation. Charge equalisation using a DC-DC converter has several advantages, including compact size, minimum equalisation time, high equalisation efficiency, and low cost [17, 18]. According to the available literature, this section will provide a comprehensive overview of various DC-DC converter topologies. The DC-DC converter will function with the required energy flow modes to transfer energy from the battery pack to the cell or cell to the battery pack, which are also covered in this section.

3.1. Various Energy Flow Techniques. Different energy flow techniques can achieve active cell balancing, including cell-to-cell, cell-to-pack, and pack-to-cell. This section discusses the benefits and drawbacks of energy flow techniques.

Cell-to-cell energy flow technique:

Cell-to-cell energy flow technique

The charge equalisation between adjacent cells is accomplished using the cell-to-cell energy flow technique. This method uses a conventional DC/DC converter circuit with an array of selection switches. The main benefit is that it has a faster balancing speed; however, the balancing circuit has far too many switching elements, resulting in low equalising efficiency [19].

Cell-to-pack energy flow technique:

Cell to pack energy flow technique

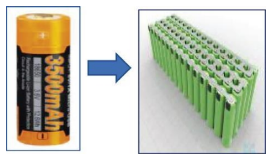

The cell-to-pack approach uses a single DC-DC converter to transfer energy from an overcharged cell to the entire battery pack. Due to transformer losses, the cell-to-pack technique has a low balancing efficiency. However, due to the considerable voltage difference between a cell and the battery pack, the equalisation speed is often high compared to alternative techniques [20].

Pack-to-cell energy flow technique:

Pack to cell energy flow technique

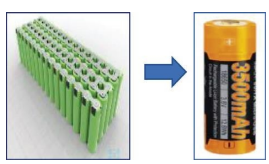

The charge is transferred from the pack to the undercharged cell in the battery pack using the pack-to-cell energy transfer technique. The DC-DC converter's terminals (input/output) are linked to the battery pack and identified cell, respectively. The pack-to-cell approach has nearly identical characteristics to the cell-to-pack technique [21].

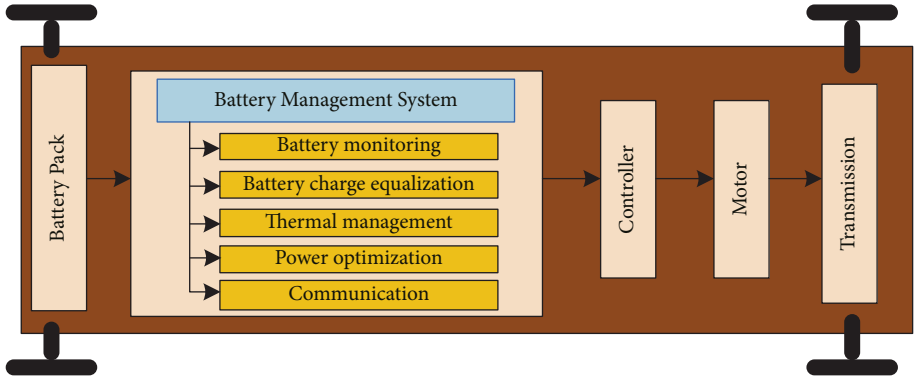

Figure 4: The module EV with the BCE system.

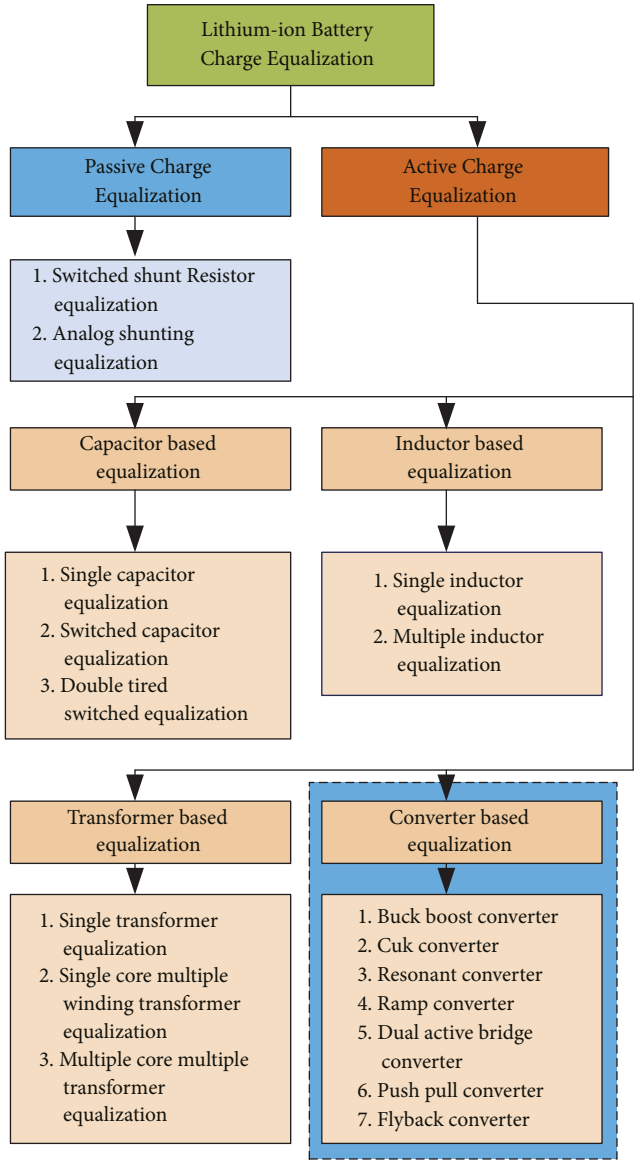

Figure 5: Classification of BEC topologies.

3.2. Various DC-DC Converter Topologies. The DC-DC converter is crucial for charge equalisation. It transfers energy from one cell to the whole pack and vice versa. For the cell-to-pack and pack-to-cell equalisation, high voltage rating converters are used. For cell-to-cell equalisation, low voltage rating converters are utilised. There are two types of converters: one based on energy transmission (unidirectional and bidirectional converters) and the other based on isolation between source and load (non-isolated and isolated converters) [22]. A unidirectional converter transfers power only in one direction, from source to load, whereas a bidirectional converter transfers power in both directions, from source to load and vice versa. The buck, boost, and Cuk converters are nonisolated since there is no isolation between source and load. Isolated converters provide electric isolation between source and load via an isolation transformer; examples include flyback, push-pull, and dual active bridge converters [23].

The design of DC-DC converters will be handled with extreme caution. The number of electrical components employed, electric isolation, energy transferring efficiency, power rating, and voltage ratio are some of the criteria considered. These factors must be carefully examined during the design process, or the circuit's complexity, cost, and size may be severely impacted [24]. This section describes the many DC-DC converter topologies used for battery charge equalisation, including design parameters and operation. Buck-boost, Cuk, ramp, resonant, dual active bridge, push-pull, and flyback converters are all considered [25].

3.2.1. Buck-Boost Converter Equalisation. Buck-boost converters are frequently used to increase or decrease the supply voltage. Several topologies based on buck-boost converters allow the buck-boost converter to transfer excess energy from overcharged cells to the DC link and then back to the undercharged cells for equalisation. The buck-boost converter topology is given in Figure 6 [26, 27]. This topology has $N-1$ buck-boost converters for N number of cells, $2N-2$ switches, and $N-1$ inductors. The energy will be stored in the corresponding inductor when the switches of highly charged battery cells are turned on for equalisation. The switch will cut off when the inductor reaches its maximum current. The inductor's stored energy is then transmitted to the undercharged cell, turning it on. This process will continue until the state of equalisation is achieved [28].

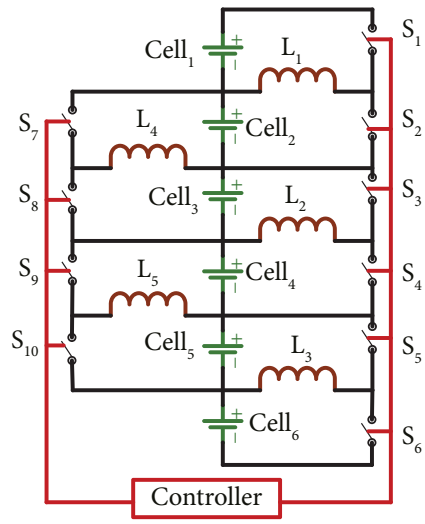

Figure 6: Buck-boost converter-based BCE.

Unlike a traditional buck-boost converter, a balanced topology is proposed that uses only one MOSFET per cell to maximise overall efficiency while lowering circuit cost. On the other hand, control complexity has skyrocketed [29]. An isolated buck-boost converter with a transformer rather than a coil is proposed to provide isolation between battery cells. This improved the circuit's ability to protect itself by preventing errors from spreading to other series-connected cells [30]. As an alternative to the traditional kind, a buck-boost converter with four switches is employed [31].

The equalisation should have a cell voltage sensing module and an intelligent control technique to operate this converter [32] properly. The duty cycle obtained by computing the voltage difference will control the energy transmission of this equalisation. This equaliser can also be used in a modular setting. The critical constraint of equalisation is the relatively expensive cost due to the numerous components used and the complexity of the voltage sensing and control technique [33].

Individual cell balancing is possible using buck-boost converter-based balancing topologies, and execution is easy. The voltage at the buck-boost converters' terminals is at its highest. As a result, the power rate is meagre and power loss is minimal. However, due to a large number of converter circuits, it has a slow balancing speed and a high cost and bulk [34]. The following equation calculates the inductance value of the buck-boost converter.

$$L = \frac{UT_s}{\Delta i_L} D, \tag{1}$$

where U is the average voltage of cells, T_s is the switching period, Δi_L is the inductance ripple current, and D is the duty cycle.

3.2.2. Cuk Converter. The traditional Cuk converter circuit is shown in Figure 7. A Cuk converter comprises two inductors, one capacitor, and two switches. For equalisation, $N-1$ number of Cuk converters are needed for balancing N number of cells; hence, totally, $2N-2$ switches, $2N-2$ inductors, and $N-1$ capacitors are required for this topology. The operating concept is similar to that of a buck-boost converter with one exception: in a buck-boost converter, the inductor participates in energy transfer, but in a Cuk converter, the capacitor does [35, 36].

If the voltage in cell 1 exceeds the voltage in cell 2, the excess voltage in cell one is transferred to cell 2 for equalisation. When switch $S1$ is closed, the capacitor $C1$ voltage is discharged to cell 2. Then, in the next pulse period, switches $S1$ and $S2$ are opened and closed, causing the excessive voltage in cell 1 to be charged in $C1$ via inductor $L1$ [37]. The creation of the adaptive sliding-mode control (SMC) scheme is offered after the study and modelling of the modified isolated Cuk-based equalisation. The proposed technique can deal with external disturbances and changes in system characteristics [38].

To increase the equalisation speed, the suggested equalisation used coupled inductor rather than a traditional uncoupled inductor. The uncoupled inductor takes longer to equalise over long string cells, which is overcome by the coupled inductor [39]. A fuzzy con-equalisation was proposed for the Cuk converter to tune the equalisation current. Multi-indices such as equalising speed, efficiency, and cell protection are used to assess the overall performance of the suggested equaliser [40].

Only n switches are needed to implement the suggested buck-boost with the Cuk converter. Unlike the other existing topologies, it achieves nearly half the switch count reduction without sacrificing modularity or device voltage stress [41]. The balancing circuit for the Cuk converter offers all of the benefits of a cell-to-cell charge transfer topology. In addition, a capacitor is less expensive than an inductor for energy storage. The input and output currents have a low level of ripple. On the other hand, the number of circuit components increases the topology volume [42, 43]. The following equation gives the inductance and capacitance values of the Cuk converter.

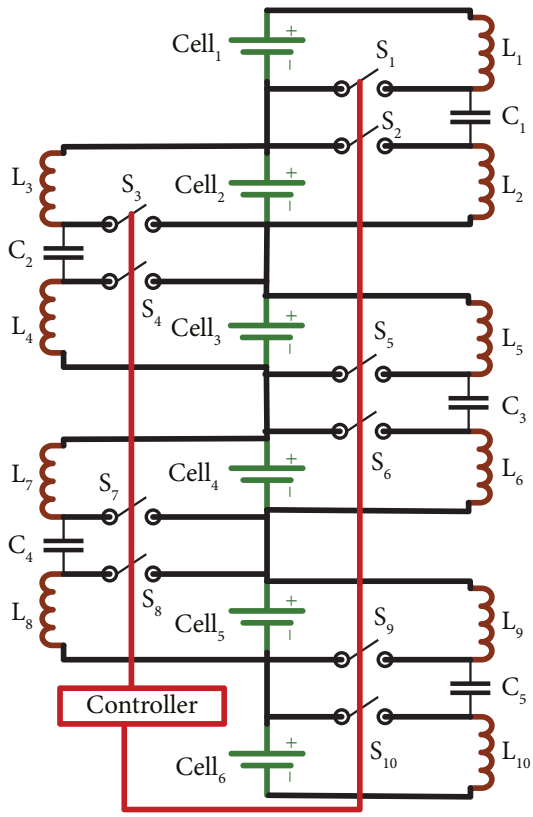

Figure 7: Cuk converter-based BCE.

$$L = \frac{DV_{\text{in}}}{\Delta L_i f_s},$$
$$C = \frac{DI_{\text{dc}}}{\Delta V_c f_s}, \tag{2}$$

where D is the duty ratio, V_{in} is the input voltage, ΔL_i is the input inductance current ripple, f_s is the switching frequency, I_{dc} is the output current, and ΔV_c is the capacitor voltage ripple.

3.2.3. Resonant Converter. The use of resonant converter circuits decreases switching losses. Because of the deep tank in their structure, which is made up of an inductor and a capacitor coupled in series or parallel, it reduces switching losses by constraining current and voltage rising speed during the turn-on and turn-off procedures of the switching components. [44]. The basic resonant converter topology for BCE is shown in Figure 8, with $2N-2$ switches, $2N-2$ inductors, and $N-1$ capacitors for the N number of cells. The controller oversees the conduction switch. By restricting the current value, the resonant tank reduces switching losses and voltage rising time by connecting inductors and capacitors in series and parallel [45]. With a voltage difference between two cells, the resonance circuit will work. The inductor can transfer energy from an overcharged cell to an undercharged cell [46].

This research presented a novel bipolar resonant LC converter (BRLCC) for multi-cell to multi-cell topology to increase equalisation speed and efficiency. The BRLCC employs the bipolar resonance of the LC deep tank to distribute energy in a fast mode, expanding the equalisation speed. However, this topology is challenging to create and operate due to the vast number of inductors and capacitors [47]. This study proposes a Lithium-Ion battery module active cell-to-cell balancing circuit. An LLC resonant converter transmits the surplus charge directly from the overcharged cell to the undercharged cell. All the primary switches in the converter are designed to operate at almost zero voltage and current. Because the number of buttons in this circuit is decreased, this topology can achieve high efficiency and rapid equalisation speed while requiring minimal control and design. However, the topology has a considerable switching loss [48].

A systematic approach is presented in this study for reforming and analysing a soft-switching bidirectional dc-dc converter. The quasi-resonant converter circuit was constructed to eliminate losses and achieve zero switching. As a result, switching losses can be reduced, improving energy transfer efficiency [49]. Due to the reduction in switching losses, the resonant converter-based battery charge equalisation architecture offers high efficiency; nevertheless, the design cost and implementation difficulty are considerable [50], four. The inductance and capacitance modelling are as follows:

$$L_r = \frac{1}{4\pi^2 C_r f_s^2},$$
$$L_m = \frac{V_0 D}{4V_{\text{in}} f_s}, \tag{3}$$
$$C_r = \frac{1}{(2\pi f_s)^2 L_r},$$

where L_r is the resonance inducsizingetizing inductance, C_r is the resonance capacitance, f_s is the resonance frequency, V_0 is the output voltage, D is the duty ratio, and V_{in} is the input voltage.

3.2.4. Ramp Converter. The ramp converter is the next generation of multi-winding transformer charge equalisation. The ramp circuit comprises a multi-winding transformer, as shown in Figure 9. The transformer's secondary winding is connected to the battery pack. This topology includes N number of switches, $N/2$ inductors, N capacitors, and N diodes for N number of cells [51, 52]. The ramp converter can work as follows: during the first cycle, the excess energy can be transferred from the cell to the battery pack through a capacitor and transformer for equalisation. In the second cycle, the power will move from the battery pack to a cell under charge through a transformer and a capacitor [53].

Soft switching is used for all switching devices during turn ON and OFF operations to diminish switching losses and improve efficiency. Due to the smaller number of windings, ramp converter-based charge equalisation is the most cost-effective. One of the primary advantages of this design is that leakage inductance is avoided. Although the

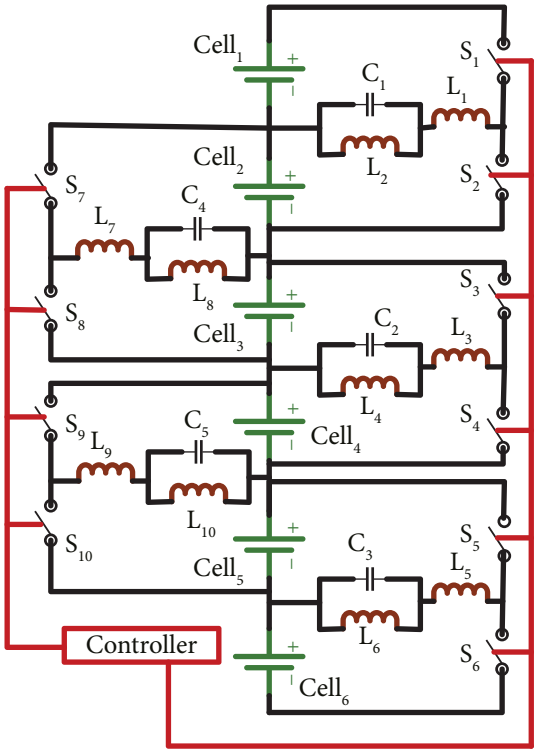

Figure 8: Resonant converter-based BCE.

cost i lower, the circuit design is more complex [54]. The inductance and capacitance values are calculated by.

$$L = \frac{V_0(1-D)}{f_s \Delta L_i},$$
$$C = \frac{1-D}{(\Delta V_c/V_0)8L(f_s)^2}, \tag{4}$$

where V_0 is the output voltage, D is the duty ratio, f_s is the switching frequency, ΔL_i is the inductance current ripple, and ΔV_c is is the capacitor voltage ripple.

3.2.5. Push-Pull Converter. The push-pull converter is one of the isolated converters, and there is galvanic isolation between source and load. The basic architecture of this converter is illustrated in Figure 10. For N number of cells, this topology consists of $2N+4$ switches, two diodes, one capacitor, and one transformer [54, 55]. Cell-to-cell, cell-to-pack, and pack-to-cell energy transfer systems can be possible with a push-pull converter polarisation to adjust the polarisation of voltage that will impact the transformer's primary winding in response to the trigger signal. This voltage is a periodic pulse waveform with appropriate switching signals. This voltage waveform is rectified and sent to the output by secondary diodes. The full-bridge and half-bridge converters operate similarly [56, 57].

The active clamp push-pull converter is proposed in [58], with switching losses decreased and conversion efficiency improved because the primary and secondary switches are turned on with zero voltage switching. Furthermore, the

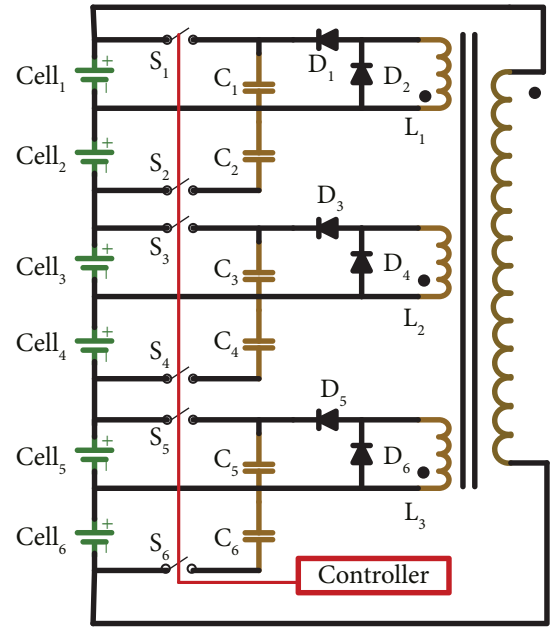

Figure 9: Ramp converter-based BCE.

proposed converter can minimise imbalance issues with traditional push-pull converters [59]. A charge equalisation for series-connected battery strings is provided in this work, which is based on a current-fed-push-pull converter and the AC-link approach. With the AC-link approach, the suggested charge equalisation may redistribute energy directly between the battery pack and achieve balance rapidly through a simple control. Energy conversion efficiency can be improved slightly by removing the rectifier diodes. [60]. The inductance and capacitance values of the push-pull converter are calculated using the equation below.

$$L = \frac{V_0(1-D)}{\Delta L_i \times 7},$$
$$C = \frac{(1-2\ D)}{32 f_s^2 L} \times \frac{V_i}{\Delta V_0}, \tag{5}$$

where V_0 is the output voltage, D is the duty ratio, ΔL_i is the input inductance current ripple, V_i is the input voltage, f_s is the switching frequency, and ΔV_0 is the output voltage ripple.

3.2.6. Dual Active Bridge Rectifier. The dual active bridge (DAB) converter is also one of the isolated converters. The significant advantages of this converter are galvanic isolation, excellent power transfer capabilities, and a wide voltage range. The DAB converter's basic design is shown in Figure 11. [60]. This architecture has one DAB converter, $2N$ switches, two diodes, and one transformer for N number of cells. Two H bridges with four buttons on either side of the transformer make up the DAB converter. The transformer is utilised for galvanic isolation and voltage synchronisation between the low and high-voltage sides of the transformer [61].

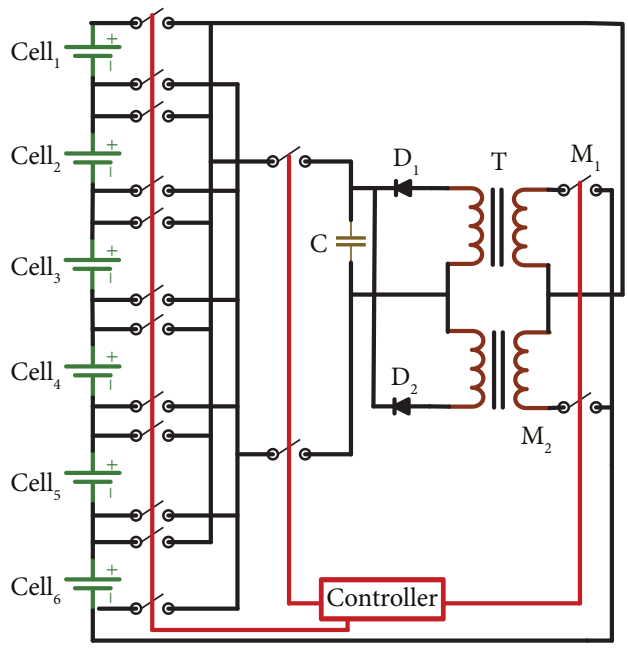

Figure 10: Push-pull converter-based BCE.

The DAB converter supports both buck and boost modes of operation. The surplus energy is saved in the leakage inductance of a transformer. The DAB converter is appropriate for topologies such as packs to cells and vice versa. Closed-loop control keeps the current equalisation constant and enables effective charge control. This topology has a small footprint, remarkable efficiency, and excellent precision [62, 63]. Unlike other DAB-based topologies, the DAB converter is switched in the middle of each cell within a battery pack and a universal low-voltage bus in this work. The proposed technique allows easy control, but the size and expense of the balancing system have significantly risen due to the usage of N DAB converters for the N number of cells [64]. The DAB converter-based equalisation architecture is ideally suited for battery packs with N number of cells and offers fast balancing, but it is a heavy and expected site. The capacitance value of the dual active bridge converter is given by.

$$C = \frac{(1 - 2\ D)}{f_s^2} \times \frac{V_0}{\Delta V_0}, \tag{6}$$

where D is the duty ratio, V_0 is the output voltage, f_s is the resonance frequency, and ΔV_0 is the output voltage ripple.

3.2.7. Flyback Converter. A flyback converter is an isolated type of converter. A buck-boost converter is used to create it. The magnetisation inductance of the transformer is used as a storage element; for N number of cells, $2N+4$ number of switches, two capacitors and one transformer are used in this topology for BCE. This topology is depicted in the circuit shown in Figure 12 [65, 66]. The flyback converter can operate in unidirectional as well as bidirectional modes. A single switch is used for energy transfer in a unidirectional type, while two switches are used in a bidirectional type. An integrated flyback converter having a switching array is used to distinguish between overcharged and undercharged cells [67, 68].

When the voltage of any cell exceeds the battery pack's maximum voltage, the equalisation mode of "cells to packs" is chosen. To charge the surplus energy in the transformer's inductance, switch $M1$ is switched on, and switch $M2$ is shut off for a short period. Switch $M1$ is turned off, while switch $M2$ is switched on during the remaining switching period. The energy held in the inductance of the transformer is discharged to the battery pack, resulting in cell-to-pack equalisation. For pack-to-cell equalisation, the same procedure is followed reversely [69, 70]. This study proposed a bidirectional equalisation topology with multi-winding input and output. This topology may overcome the drawbacks of limited energy flow direction and wasteful charge transfer, but it is mainly because of the several windings and is also expensive [71].

The proposed flyback converter reduces the battery pack's consistency. The energy transfer between the battery pack and any individual cell is accomplished using a flyback converter with a simple and reliable structure. The number of materials and size of the system could be reduced by using this topology [69, 72]. The balancing topology based on flyback converters has fewer circuit components, which decreases circuit complexity. It also includes all the benefits of a cell to pack and pack-to-cell equalisation. However, because of the transformer, the circuit size is more significant than buck-boost and Cuk converter types, increasing the cost [73, 74]. The capacitance value of the flyback converter is calculated as follows.

$$C = \frac{D}{Rf_s} \times \frac{V_0}{\Delta V_0}, \tag{7}$$

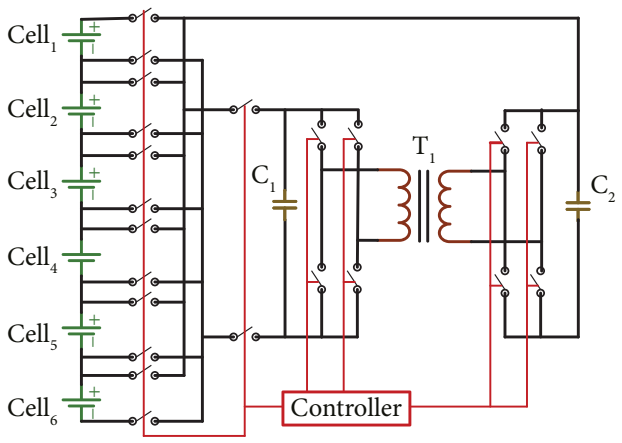

Figure 11: Dual active bridge converter-based BCE.

where D is the duty ratio, V_0 is the output voltage, R is the load resistance, f_s is the resonance frequency, and ΔV_0 is the output voltage ripple.

4. Control Strategies of DC-DC Converter-Based BCE

The control strategies of the DC-DC converter are a software part of the BCE system. A mathematical formulation of the equalisation system can help to develop control strategies. The control techniques' major goal is to offer stability and better operation while reducing inconsistency in battery cells with minimal balancing time and power loss. The output of the BCE system is used to define the mathematical model; the system output is the balancing current that passes through the converter at the time of balancing operation. Electrical circuit components such as resister inductors, capacitators, and controller characteristics such as PWM signal duty cycle and switching frequency are defined. Control strategy classification for control variables is briefly covered in this section [75, 76].

4.1. Classification of Control Strategies by Control Variables. The control variables, which constitute the control strategy's input, provide information about the battery packs and cells. Terminal voltage, OCV, SOC, and capacity are examples. Decorticating the input variable is the key component that directly influences the accuracy of balancing schemes. Control variables, as well as their benefits and drawbacks, are examined in this section. The classification of control strategies by control variables is shown in Figure 13.

4.2. Cell Voltage-Based Control Strategy. Cell voltage-based equalisation has a solution that transfers energy among cells based on their voltage differential. The balancing procedure begins with the BEC system evaluating the differences between the cell's voltage and the threshold voltage. If the discrepancies exceed the pre-set value, the battery pack will charge cells with under-voltage through the cells with

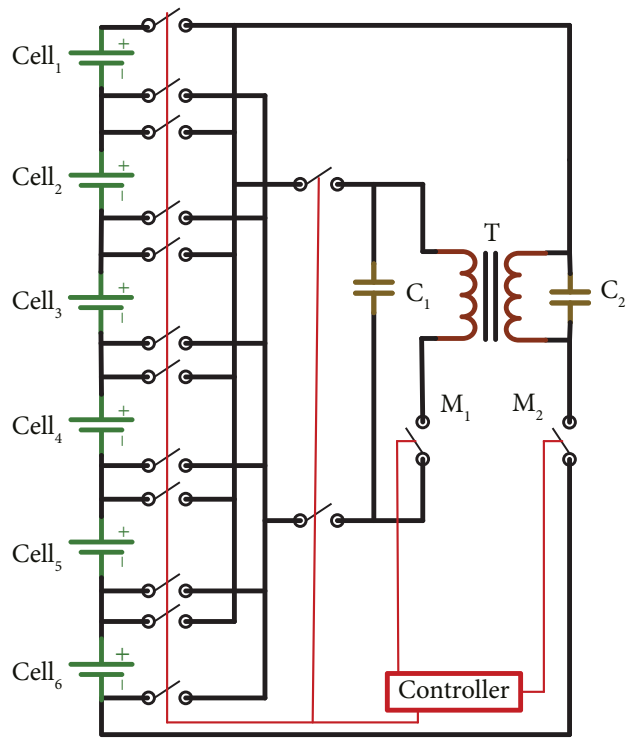

Figure 12: Flyback converter-based BCE.

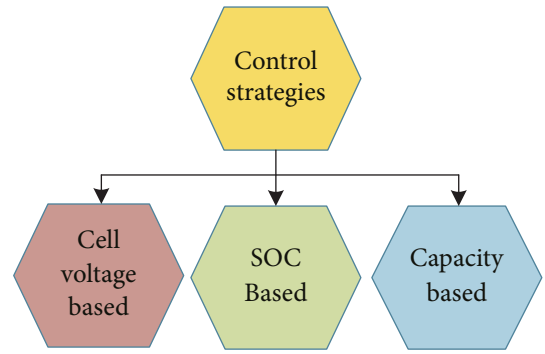

Figure 13: Classification of control strategies.

overvoltage [77]. Control techniques based on terminal voltage balancing are simple to implement because the voltage is measured immediately throughout the balancing process. However, this method causes a few errors in the cell's internal resistance and decreases battery capacity, mainly due to the ageing effect of the battery. With the aid of the Thevenin equivalent circuit, the battery terminal voltage is expressed by open-circuit voltage, voltage losses on internal resistance, and polarisation voltage [78]. There is a link between OCV and SOC, which indicates that cells with similar SOCs have nearly identical OCVs. On the other hand, inconsistencies in internal resistance cause differences in terminal voltages among cells, even if their SOCs are equal. The charging voltage cell curve theory was developed to overcome the limitations of voltage-based control techniques. Additionally, the battery pack's capacity is maximised [79].

4.3. Capacity-Based Control Strategies. The battery's charging, discharging, and overall capacity are input variables in capacity-based balancing schemes. Even though the SOC and voltage of the cells are equivalent, internal resistance with capacity variances causes the dischargeable capacities of these cells to differ. When the battery hits the maximum voltage, the cell with the highest capacity will have the most residual capacity. As a result, the battery's energy use efficiency will decrease, and its life cycle will be shortened [80]. The capacity of cells was used as a control variable in this paper, and the equalisation current was tested. According to the experimental results, the algorithm of voltage-based balancing and the suggested control method were compared, and finally concluded that using capacity as a control variable can improve the charging capacity [81].

Capacity-based control strategies offer numerous benefits. Initially, it maximises energy efficiency. The *m* Maximum usable capacity can extend the battery's overall life, which is critical for providing cost-effective EVs. However, determining each cell's ability in real-time places a computational load on BMS's hardware component. The requirement for SOC data to estimate capacity will add to the computational complexity [82].

4.4. SOC-Based Control Strategies. The SOC status of the battery cell is used as an input variable in SOC-based balancing techniques. During both charges and the discharge process, it moves energy from the cell with the highest SOC to the cell with the lowest SOC [83]. It provides more precise balancing compared to terminal voltage-based techniques because of the strong correlation between open-circuit voltage, which reflects the internal status of the battery, and SOC. Furthermore, even if total capacity differences exist across cells, SOC-based balancing control algorithms ensure that the cells are fully charged or fully discharged, allowing the entire pack's energy to be utilised [84].

SOC is the ratio of the battery's dischargeable capacity to its nominal capacity, and it cannot be directly measured with a sensor; hence several SOC estimation methods are proposed [85]. These strategies can be divided into four categories for comparison and analysis, [86]. The SOC estimate approach is used for the BCE process when employing a DC-DC converter. SOC is determined for each cell and kept as balanced control parameters. During the initialisation phase, the bubble approach calculates the highest SOC value (*C*max) and the minimum SOC value (SOC_{min}). If the SOC_{min} is less than the pre-set SOC for a start balancing (SOC_{set}), the iteration is continued; otherwise, the titration is stopped, and a restart increment is made. The following equation calcifies SOC [87, 88].

$$\begin{aligned} \Delta SOC &= SOC_{max} - \sum_{n-1}^{N} \frac{SOC_n}{N}, \\ SOC &= \sum_{n-1}^{N} \frac{SOC_n}{N}. \end{aligned} \tag{8}$$

If SOC is less than the SOC_{set} for commencing balancing, the iteration is resumed; otherwise, it is finished and restarted after a pre-determined time. The battery supplies the energy to the transformer. In this process, the reduced SOC of battery *n* is denoted by SOC_n and calculated as follows [89]:

$$\Delta'_{SOC} n = \frac{\int i_{dt}}{C_{bat}, n}, \tag{9}$$

where C_{bat} stands for the battery's overall capacity and "*I*" stands for the battery current. The positive current flows through the battery's outlet's positive electrode. When the difference between Δ_{SOC}' and Δ_{SOC} is less than a number but greater than zero, the drive signal of the relevant power tube is set to "low" and the iteration is resumed and reinitialised. The control strategy flowchart in Figure 14 depicts a step-by-step approach to SOC estimation [90, 91].

4.4.1. Various Methods of SOC Estimation. One of the most significant components of a battery charge equalisation system is the SOC estimation. A large variety of SOC estimating algorithms have been presented for real time applications. For optimal design and efficient energy transfer, proper SOC estimation is required. Figure 15 depicts various approaches for estimating SOC.

(1) Direct Measurement Method. The physical parameters of the battery, such as impedance and terminal voltages, are factored into the direct measurement method. The open circuit voltage method (OCV), terminal voltage (TV) methods, impedance methods, and impedance spectroscopy (IS) methods are the most popular approaches. Table 3 compares the various methods of direct measurement.

(2) Bookkeeping Methods. This approach estimates the SOC using the battery discharge current data as an input. Internal battery impacts such as capacity loss, self-discharge, and discharging efficiency will influence these strategies. The Coulomb counting (CC) and modified Coulomb counting (MCC) methods are included in this method. Table 4 compares several systems of bookkeeping procedures.

(3) Adaptive Methods. With the advancement of artificial intelligence, the adaptive method of SOC estimation was developed. The adaptive technique delivers excellent accuracy and robustness when estimating battery SOC. It has a unique self-correcting characteristic that compensates for variations in input signals. Neural network (NN) and support vector machine (SVM) are two popular methods. Others include Kalman filter (KF), extended Kalman filter (EKF), and fuzzy neural network (FNN) method. The comparison of several adaptive strategies is shown in Table 5.

(4) Hybrid Model. This approach will utilise the advantages of the abovementioned methods to achieve maximum estimation performance and increase estimating accuracy. Coulomb counting and EMF (CC&EMF), Coulomb counting and Kalman filter (CC&KF), and per-unit system

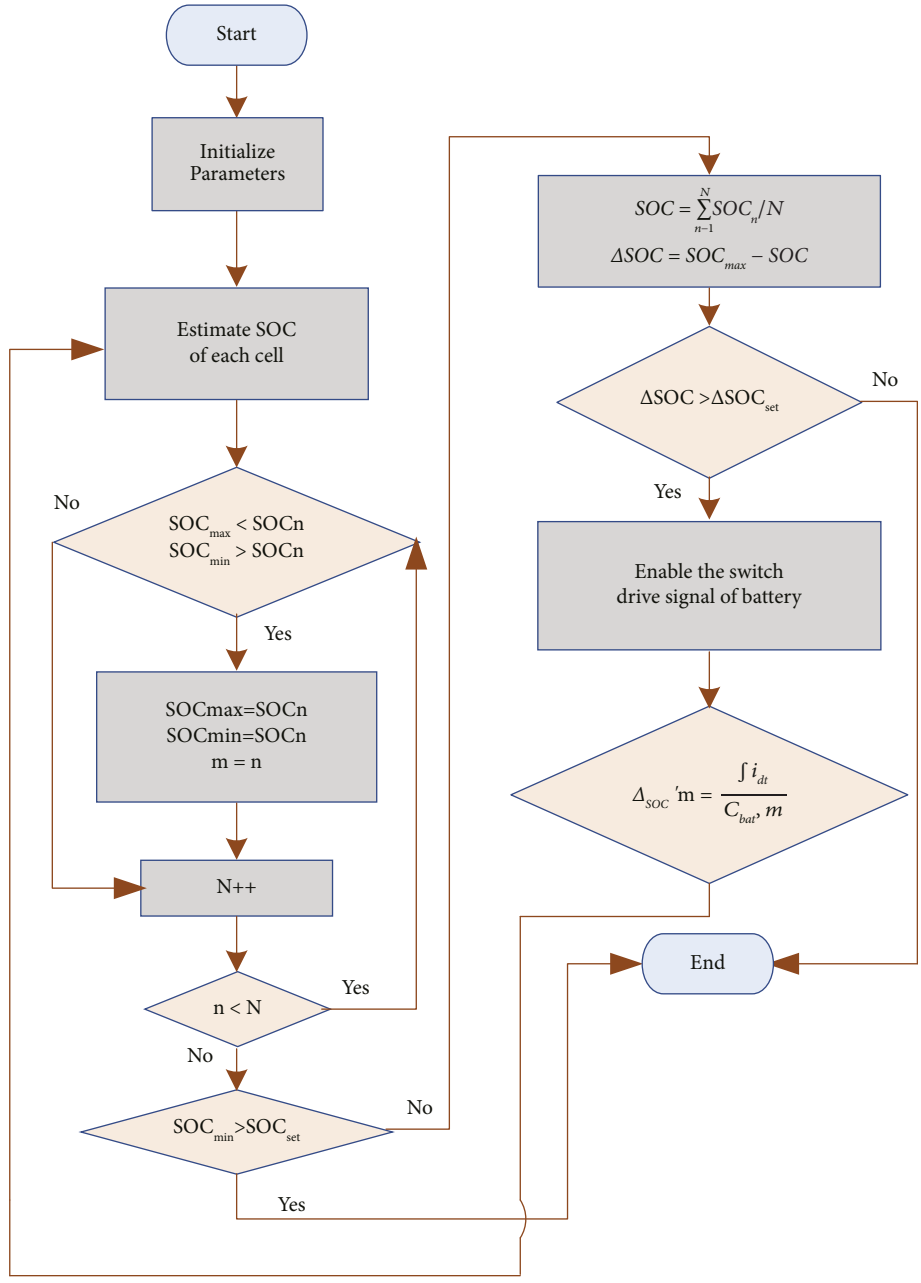

Figure 14: SOC estimation flow chart.

and EKF (PUS & EKF) are some of the most frequent hybrid models. Table 6 shows a comparison of various hybrid models.

Various SOC estimating strategies are thoroughly compared in the section above. The methods have a few flaws in at least one area, such as poor accuracy, implementation issues, sensor drifts, complicated programming, huge memory capacity, and complex computing. Researchers are still working on providing a suitable SOC estimating approach to address the flaws above. Whatever the new idea is, it will only be employed at the laboratory level; meanwhile, classic techniques like direct measurement and bookkeeping methods are nearly always used in EV applications [105], [106].

5. Analysis of DC-DC Converter-Based BCE with Its Control Strategies

The topologies of DC-DC converters for cell balancing were investigated using MATLAB Simulink, with six cells connected in series performing the analysis. The following section includes the critical modelling parameters for each partition: inductance and capacitance values, duty cycle, and initial SOC value. Because of the difference in the number of cells used, several parameters differ from those in the literature. This section discusses converter performance balancing time, cost, size, and efficiency, as well as simulation results for various converter topologies for BCE.

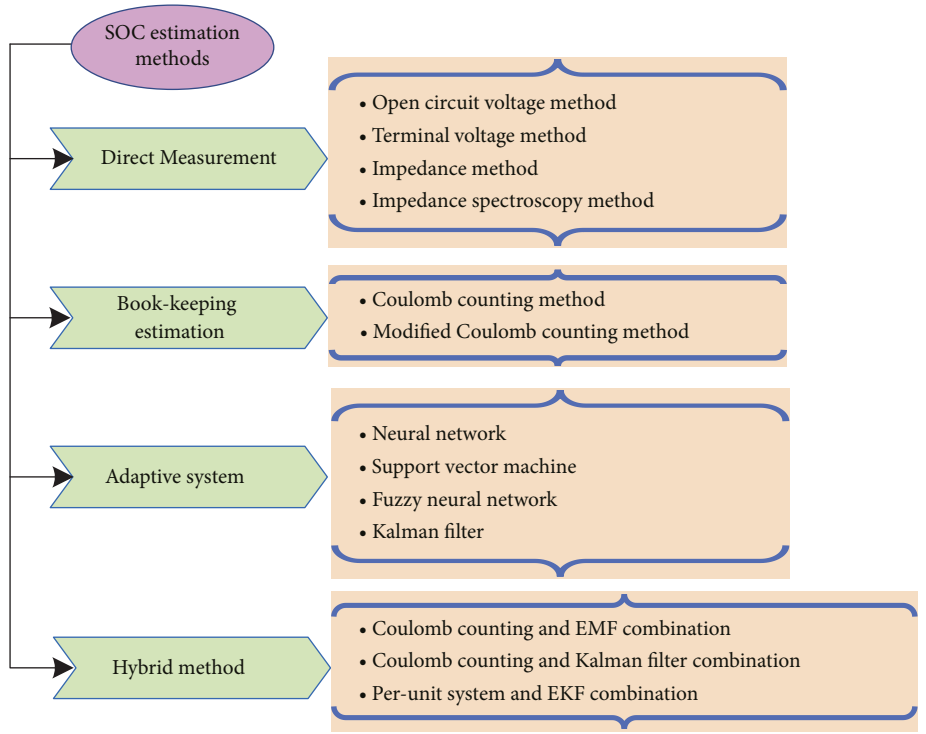

Figure 15: Methods of SOC estimation.

Table 3: Comparison of the direct measurement method of SOC estimation.

Methods	Principle	Merits	Demerits
OCV [92]	SOC and OCV have a linear relationship. This will be accomplished by putting a pulse load on the battery and then allowing it to stabilise. Depending on the battery, this relationship will change.	(i) Simple method (ii) Cost-effective (iii) Easy implementation	(i) Long time required for equilibrium (ii) Less accuracy
TV [93]	Internal impedance causes the terminal voltage of the battery to decline; the terminal voltage is proportional to the electrical motive force (EMF), which is proportional to the state of charge (SOC). As a result, the terminal voltage can be used to calculate SOC.	(i) Simple method (ii) Suitable for all batteries	(i) The error will occur due to a sudden voltage drop at the discharge end
Impedance [94]	Internal resistance is measured using the battery voltage and current in this manner. The internal resistance value is calculated using the voltage and current ratio to estimate SOC.	(i) Very flexible (ii) Easy implementation	(i) Less accuracy (ii) Very difficult to observe when a slight change in internal resistance causes wide variation in SOC
IS [95]	To assess impedance, multiple frequencies are applied across the battery. SOC is calculated using this impedance.	(i) Suitable for online estimation (ii) Low cost (iii) Good accuracy	(i) The battery temperature and ageing will affect the assessment

Table 4: Comparison of bookkeeping method of SOC estimation.

Methods	Principle	Merits	Demerits
CC [96]	This method estimates SOC by measuring the discharging current first and then integrating it with time. The SOC (t) is calculated by discharging current I (t).	(i) Low power consumption (ii) Easy implementation	(i) Less accuracy (ii) Difficult to define initial SOC values
MCC [97]	This approach improves estimation accuracy by using rectified current values. The function of discharging current is the rectified current. Corrected current and discharging current have a quadratic connection.	(i) More accuracy (ii) Low power consumption (iii) Easy implementation	(i) Highly depend on discharging current

Table 5: Comparison of an adaptive method of SOC estimation.

Methods	Principle	Merits	Demerits
NN [98]	NN is a framework for many machine learning algorithms to fulfil various tasks. The highly complex and nonlinear system can be handled using NN. SOC estimation is based on the training data used in NN, wh measured by experiments on charging and discharging batteries.	(i) Simple method (ii) Minimum error (iii) Solve nonlinear system	(i) The error will increase if enough trained data is not available (ii) Need bulky memory unit
SVM [99]	In numerous domains of pattern recognition, SVM is used to classify data. Regression problems can also be solved with SVM. It's capable of dealing with nonlinear systems.	(i) Simple method (ii) More robust	(i) Insensitive to small changes in the input signal
FNN [100]	FNN is used to identify unknown systems. FNN can handle nonlinear systems by finding the learning mechanism's optimal coefficient.	(i) Very effective (ii) High performance	(i) Complex computation (ii) Costly (iii) Need bulky memory unit
KF [101]	KF is a valuable method for estimating SOC for a battery in real-time state estimation, and it's also used to estimate the state of a dynamic system. The extended kalman filter (EKF) is a KF enhancement. A nonlinearization method expanded the nonlinear system dynamics and model measurement. This will increase the accuracy of SOC estimation.	(i) Self-correcting nature (ii) More accuracy (iii) Solve nonlinear dynamic errors	(i) Complex calculation (ii) Linearization error will occur

Table 6: Comparison of the hybrid model of SOC estimation.

Methods	Principle	Merits	Demerits
CC & EMF [102]	This approach will use the direct measurement method with EMF measurement during the equilibrium state and the bookkeeping estimating method with the CC method during the discharging state.	(i) More accuracy (ii) Solving nonlinear system	(i) Limited robustness (ii) Linearization error will occur
CC & KF [103]	It employs the KF method to fix the CC method's initial values. This method yielded an approximation beginning value that convenes a real deal and SOC estimation for the prolonged working duration.	(i) Low power consumption (ii) Self-correcting nature	(i) Complex calculation (ii) Inaccurate outcomes
PUS & EKF [104]	This combination is used to find the best battery model parameter for calculating SOC with high accuracy. Parameters' absolute values are converted to dimensionless values about a set of base values.	(i) Predicts nonlinear errors (ii) More accuracy	(i) Complex program (ii) Bulky memory

5.1. Simulation Parameters of DC-DC Converters for BCE. Table 7 lists the specifications of a lithium-ion battery, including the number of cells, nominal voltage, maximum charging voltage, standard discharging current, internal resistance, maximum useable capacity, and life cycle. Table 8 shows the components needed to design DC-DC converters for BCE. The values are based on past literature, with certain exceptions made on the basis of simulation results [107].

5.2. Initial SOC Values of Each Cell in the Lithium-Ion Battery Pack. The cell imbalance is identified by measuring the cell SOC. SOC-based balancing takes less time than voltage-based balancing. The initial SOC values of six cells connected in series are shown in Table 9. Assumptions are made based on the original SOC values. A MATLAB function tool was used to determine the difference in SOC values between each cell, and matching switches were turned ON or OFF based on the SOC values. The tiny variation in SOC values is also detected and triggers the balancing procedure to achieve 100% SOC. This boosts the overall efficiency of the battery pack while simultaneously increasing its capacity. The starting SOC values are assumed randomly, ranging from 70% to 90%.

Table 7: Lithium-ion battery pack specification.

Parameters	Values
Number of cells in battery pack	Six cells
Nominal voltage	3.6 V
Battery capacity	5.4 Ah
Maximum charge voltage	4.3 V
Standard discharge current	1.32 A
Internal resistance	0.014
Maximum usable capacity	2.4 Ah–19 Ah
Life cycle at dead of discharge	2000 cycles

Table 8: Components required for designing DC-DC converters for N number of cells.

	Switch	Capacitor	Inductor	Transformer	Diode
Buck-boost	$2N-2$	—	$N-1$	—	—
Cuk	$2N-2$	$N-1$	$2N-2$	—	—
Resonant	$2N-2$	$N-1$	$2N-2$	—	—
Ramp	N	N	$N/2$	—	N
Push-pull	$2N+4$	1	—	1	2
Dual active bridge	$2N+6$	2	—	1	—
Flyback	$2N+4$	2	1	1	—

Table 9: Initial SOC values of different cells.

	Cell 1 (%)	Cell 2 (%)	Cell 3 (%)	Cell 4 (%)	Cell 5 (%)	Cell 6 (%)
For all DC-DC converters	72	88	85	60	65	80

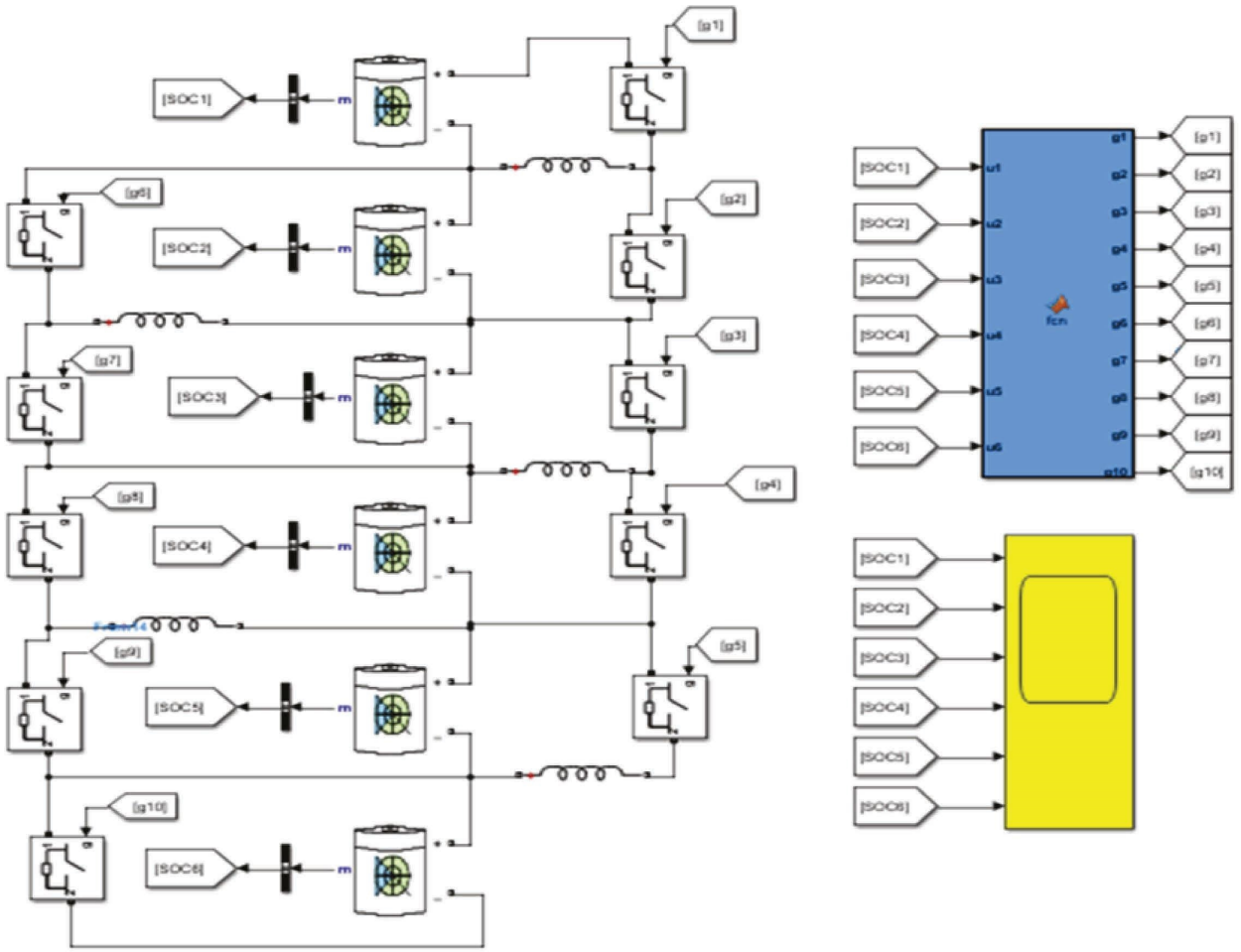

Figure 16: MATLAB simulink diagram of buck-boost converter-based BCE topology.

5.3. Simulation Results. One of the most important parameters for estimating the performance of a battery charge equalisation system is the balancing time. Other elements, like power loss and efficiency, are linked by the balancing time. The active cell balancing based the on DC-DC converter was built in MATLAB software for six cells connected in series. First, a buck-boost converter-based active cell equalisation with initial SOCs of 72%, 88%, 85%, 60%, 65%, and 80% percent was constructed and simulated for six cells. The MATLAB Simulink circuit for buck-boost converter-based BCE is shown in Figure 16. Battery parameters and quantity of electrical components needed for this topology are given in Tables 5 and 6. The inductor value is calculated from equation (1) for an average voltage of 3.6 V; the duty ratio is taken as 0.5, the switching frequency of 10 kHz, and the inductor ripple current is taken as 0.4. The parameter inductor value is obtained as 450 μH. All cells have the same capacity; hence, the exact value of the inductor is used in the entire circuit. The SOC estimation code is loaded in the MATLAB function block; the switches can operate according to the SOC values of each cell. Initially, the circuit was simulated with a minimum run time and it was increased gradually to attain the balancing state. For this circuit, all six cells are balanced after 1800 s. For other converter topologies, the same model circuit is followed; for page consideration, only one circuit is depicted in this study.

Other converters, such as Cuk, ramp, push-pull, dual active bridge, and flyback converters, are designed and simulated using the same initial SOC values listed in Table 7, as well as the duty ratio and switching frequency of each converter. The balancing time for these corresponding values is 3580, 2158 s, 3200 s, 2876 s, and 1120 s, respectively. The graph is given in Figure 17. The simulation of all DC-DC converter-based BCE topologies shows the balancing time is taken on the X-axis and SOC values of each cell are taken on the Y-axis. Initially, all cells have different SOC values, and after some time, all cells are balanced at one particular period that will be highlighted, and the balancing time will be displayed in the graph.

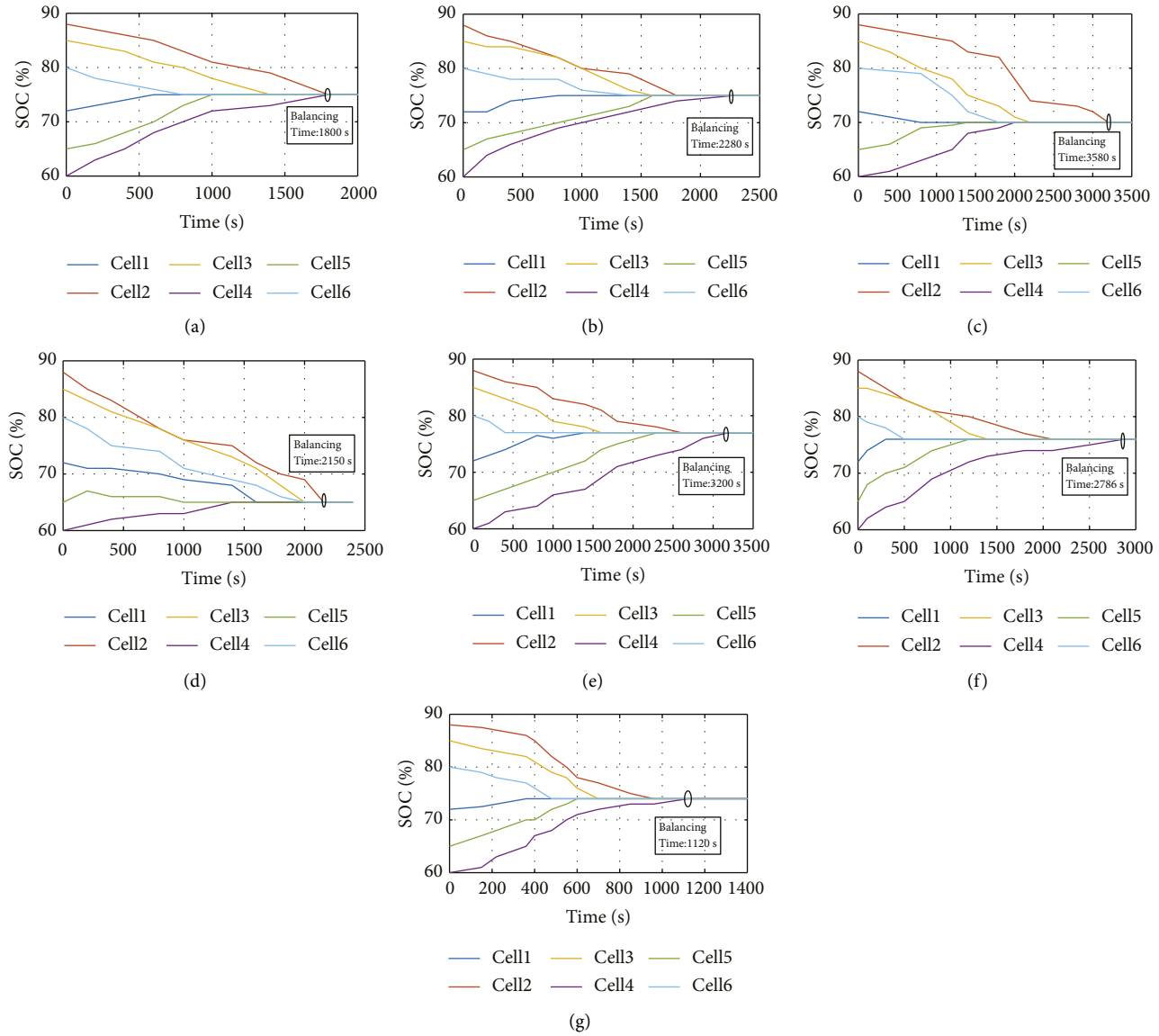

Figure 17: Simulation result for different converter topologies for cell balancing with six cells connected in series. (a) Buck-boost converter, (b) Cuk converter, (c) resonant converter, (d) ramp converter, (e) push-pull converter, (f) dual active bridge converter, and (g) flyback converter.

5.4. Comparison of Different DC-DC Converter Topologies. The comparative chart and pictorial representation of various DC-DC converter topologies and their control techniques are elaborated in Table 10 and Figure 18. This will reveal the multiple properties of DC-DC converters for BCE, such as equalisation technique, control variable, SOC estimation method, equalisation time, cost, volume, efficiency, balancing speed, control complexity, power loss, voltage, and current stress. This chart and pictorial representation make it easy to pick the suitable converter topology for BCE as per the need.

Table 10: Comparison of different converter topologies for BCE.

	Buck-boost [108, 109]	Cuk [36, 38]	Resonant [48, 110]	Ramp [15, 54]	Push-pull [57, 74]	Dual active bridge [111, 112]	Flyback [56, 113]
Equalisation techniques	DCTC	DCTC	CTP	CTP	CTPTC	CTPTC	CTPTC
Control variable	SOC	CV	CV	SOC	CV	SOC	SOC
SOC estimation	OCV	OCV	EKF	OCV	OCV	EKF	OCV
Equalisation time	The 1800 s	2280 s	3580 s	2150 s	3200 s	2786 s	1120 s
Efficiency	High	High	High	Moderate	Low	Moderate	High
Balancing speed	Fast	Medium	Slow	Medium	Slow	Medium	Fast

Note. DCTC: direct cell to cell, CTP: cell to pack, CTPTC: cell to pack to cell, SOC: state of charge, CV: cell voltage, OCV: open circuit voltage, EKF: extended kalman filter, and s: seconds.

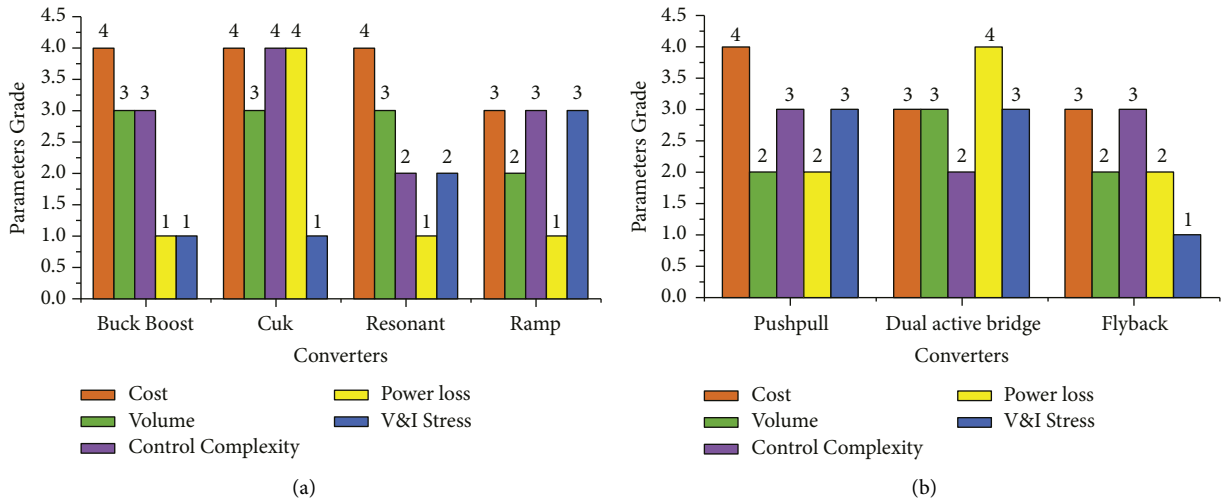

Figure 18: (a, b) Pictorial comparison of different converter topologies of BCE. Note: 1 is low, 2 is medium, 3 is high, and 4 is very high.

6. Conclusion

This article reviews a DC-DC converter-based BCE for lithium-ion battery packs from a different standpoint. The BCE techniques are greatly needed to increase the lifespan of serially connected battery cells and groups to avoid unpleasant outcomes like overcharging and undercharging. The design, operating principle, merits, and drawbacks of several DC-DC converter-based balancing topologies are discussed in this article. The numerous control tactics like the voltage, capacity, and SOC-based control strategies are described with their advantages and flaws in this article to increase the efficiency of BCE. The implementation of control strategies in BCE topologies was investigated through MATLAB simulation, and the variation of balancing speeds of different topologies was compared. Furthermore, a comparison chart and pictorial representation of several elements such as energy transfer technology, balancing time, size, cost, power loss, and efficiency were provided. The flyback converter topology has the highest balancing speed compared to other topologies (1120 s), which will be noticed in the simulation result. The comparative analysis and pictorial representation gave the flyback converter topology the highest grade. From the control strategies section, the SOC-based control strategies are highly recemented, particularly the traditional methods like direct measurement methods and bookkeeping methods, which are practically used in EV applications. Future studies will concentrate on real-time analysis for experimental validation.

Conflicts of Interest

The authors declare that they have no conflicts of interest.

References

[1] C. Acar and I. Dincer, "The potential role of hydrogen as a sustainable transportation fuel to combat global warming," *International Journal of Hydrogen Energy*, vol. 45, pp. 3396–3406, 2020.

[2] N. Niroomand, C. Bach, and M. Elser, "Segment-based CO_2 emission evaluations from passenger cars based on deep learning techniques," *IEEE Access*, vol. 9, no. 2021, pp. 166314–166327, 2021.

[3] P. Shrivastava, T. Kok Soon, M. Y. I. Bin Idris, S. Mekhilef, and S. B. R. S. Adnan, "Combined state of charge and state of energy estimation of lithium-ion battery using dual forgetting factor-based adaptive extended Kalman filter for electric vehicle applications," *IEEE Transactions on Vehicular Technology*, vol. 70, pp. 1200–1215, 2021.

[4] K. Laadjal and A. J. M. Cardoso, "Estimation of lithium-ion batteries state-condition in electric vehicle applications: issues and state of the art," *Electronics*, vol. 10, p. 1588, 2021.

[5] M. R. Khalid, A. K. Irfan, H. Salman, M. S. A. Jamil, and J. S. Ro, "A comprehensive review on structural topologies, power levels, energy storage systems, and standards for electric vehicle charging stations and their impacts on grid," *IEEE Access*, vol. 9, 2021.

[6] S. Dai, F. Zhang, and X. Zhao, "Series-connected battery equalization system: a systematic review on variables, topologies, and modular methods," *International Journal of Energy Research*, vol. 45, pp. 19709–19728, 2021.

[7] J. Xu, S. Li, C. Mi, Z. Chen, and B. Cao, "SOC based battery cell balancing with a novel topology and reduced component count," *Energies*, vol. 6, pp. 2726–2740, 2013.

[8] L. Pelletier, F. A. LeBel, C. H. Antunes, and J. P. F. Trovao, "Sizing of a battery pack based on series/parallel configurations for a high-power electric vehicle as a constrained optimization problem," *IEEE Transactions on Vehicular Technology*, vol. 69, no. 12, pp. 14150–14159, 2020.

[9] W. Diao, M. Pecht, and T. Liu, "Management of imbalances in parallel-connected lithium-ion battery packs," *Journal of Energy Storage*, vol. 24, Article ID 100781, 2019.

[10] S. Hemavathi, "Overview of cell balancing methods for Li-ion battery technology," *Energy Storage*, vol. 3, no. 2, pp. 1–12, 2020.

[11] Z. Gong, B. A. C. Van De Ven, K. M. Gupta et al., "Distributed control of active cell balancing and low-voltage bus regulation in electric vehicles using hierarchical model-predictive control," *IEEE Transactions on Industrial Electronics*, vol. 67, pp. 10464–10473, 2020.

[12] Y. Xing, E. W. M. Ma, K. L. Tsui, and M. Pecht, "Battery management systems in electric and hybrid vehicles," *Energies*, vol. 4, pp. 1840–1857, 2011.

[13] M. U. Ali, A. Zafar, S. H. Nengroo, S. Hussain, M. J. Alvi, and H. J. Kim, "Towards a smarter battery management system for electric vehicle applications: a critical review of lithium-ion battery state of charge estimation," *Energies*, vol. 12, p. 446, 2019.

[14] M. Caspar, T. Eiler, and S. Hohmann, "Systematic comparison of active balancing: a model-based quantitative analysis," *IEEE Transactions on Vehicular Technology*, vol. 67, no. 2, pp. 920–934, 2018.

[15] V. B. Vulligaddala, S. Vernekar, S. Singamla, R. K. Adusumalli, V. Ele, and M. Brandl, "A 7-cell, stackable, li-ion monitoring and active/passive balancing IC with in-built cell balancing switches for electric and hybrid vehicles," *IEEE Transactions on Industrial Informatics*, vol. 16, pp. 3335–3344, 2020.

[16] J. Carter, Z. Fan, and J. Cao, "Cell equalisation circuits: a review," *Journal of Power Sources*, vol. 448, Article ID 227489, 2020.

[17] D. Ravi, B. Mallikarjuna Reddy, and P. Samuel, "Bidirectional DC to DC converters: an overview of various topologies, switching schemes and control techniques," *International Journal of Engineering & Technology*, vol. 7, pp. 360–365, 2018.

[18] M. Raeber, A. Heinzelmann, and D. O. Abdeslam, "Analysis of an active charge balancing method based on a single nonisolated DC/DC converter," *IEEE Transactions on Industrial Electronics*, vol. 68, pp. 2257–2265, 2021.

[19] Q. Ouyang, J. Chen, J. Zheng, and Y. Hong, "SOC estimation-based quasi-sliding mode control for cell balancing in lithium-ion battery packs," *IEEE Transactions on Industrial Electronics*, vol. 65, pp. 3427–3436, 2018.

[20] A. M. Imtiaz and F. H. Khan, "Time shared flyback converter based regenerative cell balancing technique for series connected Li-ion battery strings," *IEEE Transactions on Power Electronics*, vol. 28, pp. 5960–5975, 2013.

[21] C.-H. Kim, M. Y. Kim, H. S. Park, and G. W. Moon, "A modularized two-stage charge equalizer with cell selection switches for series-connected lithium-ion battery string in an HEV," *IEEE Transactions on Power Electronics*, vol. 27, pp. 3764–3774, 2012.

[22] S. B. Tank, M. Kelvin, and A. Nitin, "Non-isolated bi-directional DC-DC converters for plug-in hybrid electric vehicle charge station application," in *Proceedings of the Emerging Trends in Computer & Electrical Engineering (ETCEE 2015)*, Kobe, Japan, November 2015.

[23] W.-Y. Choi, "High-efficiency DC–DC converter with fast dynamic response for low-voltage photovoltaic sources," *IEEE Transactions on Power Electronics*, vol. 28, pp. 706–716, 2013.

[24] M. Koseoglou, E. Tsioumas, N. Jabbour, and C. Mademlis, "Highly effective cell equalization in a lithium-ion battery management system," *IEEE Transactions on Power Electronics*, vol. 35, no. 2, pp. 2088–2099, 2020.

[25] K. Liu, K. Li, Q. Peng, and C. Zhang, "A brief review on key technologies in the battery management system of electric vehicles," *Frontiers of Mechanical Engineering*, vol. 14, pp. 47–64, 2019.

[26] F. Peng, H. Wang, and L. Yu, "Analysis and design considerations of efficiency enhanced hierarchical battery equalizer based on bipolar CCM buck-boost units," *IEEE Transactions on Industry Applications*, vol. 55, no. 4, pp. 4053–4063, 2019.

[27] M. Ohirul Qays, Y. Buswig, M. L. Hossain, and A. Abu-Siada, "Active charge balancing strategy using the state of charge estimation technique for a PV-battery hybrid system," *Energies*, vol. 13, p. 3434, 2020.

[28] X. Ding, D. Zhang, J. Cheng et al., "A novel active equalization topology for series-connected lithium-ion battery packs," *IEEE Transactions on Industry Applications*, vol. 56, pp. 6892–6903, 2020.

[29] C.-H. Kim, M.-Y. Kim, and G.-W. Moon, "A modularized charge equalizer using a battery monitoring IC for series-connected Li-ion battery strings in electric vehicles," *IEEE Transactions on Power Electronics*, vol. 28, pp. 3779–3787, 2013.

[30] Q. Ouyang, J. Chen, J. Zheng, and H. Fang, "Optimal cell-to-cell balancing topology design for serially connected lithium-ion battery packs," *IEEE Transactions on Sustainable Energy*, vol. 9, pp. 350–360, 2018.

[31] S. Yarlagadda, T. T. Hartley, and I. Husain, "A battery management system using an active charge equalization technique based on a DC/DC converter topology," *IEEE Transactions on Industry Applications*, vol. 49, no. 6, pp. 2720–2729, 2013.

[32] S. Wang, L. Kang, X. Guo, Z. Wang, and M. Liu, "A novel layered bidirectional equalizer based on a buck-boost converter for series-connected battery strings," *Energies*, vol. 10, p. 1011, 2017.

[33] M. Uno and K. Tanaka, "Single-switch cell voltage equalizer using multistacked buck-boost converters operating in discontinuous conduction mode for series-connected energy storage cells," *IEEE Transactions on Vehicular Technology*, vol. 60, pp. 3635–3645, 2011.

[34] Y. Huang, F. Liu, Y. Zhuang et al., "Bidirectional buck-boost and series LC-based power balancing units for photovoltaic DC collection system," *IEEE Journal of Emerging and Selected Topics in Power Electronics*, vol. 9, pp. 6726–6738, 2021.

[35] R. Pandey and B. Singh, "A Cuk converter and resonant LLC converter-based E-bike charger for wide output voltage variations," *IEEE Transactions on Industry Applications*, vol. 57, pp. 2682–2691, 2021.

[36] S. K. Dam and V. John, "Low-frequency selection switch-based cell-to-cell battery voltage equalizer with reduced switch count," *IEEE Transactions on Industry Applications*, vol. 57, no. 4, pp. 3842–3851, 2021.

[37] S. Dutta, S. Gangavarapu, A. K. Rathore, R. K. Singh, S. K. Mishra, and V. Khadkikar, "Novel single-phase cuk-derived bridgeless PFC converter for on-board EV charger with reduced number of components," *IEEE Transactions on Industry Applications*, vol. 58, pp. 3999–4010, 2022.

[38] H. Zhong, J. Li, and Y.-X. Wang, "A bus-based battery equalization via modified isolated cuk converter governed by adaptive control," in *Proceedings of the Chinese Automation Congress (CAC)*, Hangzhou, China, November 2019.

[39] A. Farzan Moghaddam and A. Van den Bossche, "A Ćuk converter cell balancing technique by using coupled inductors for lithium-based batteries," *Energies*, vol. 12, p. 2881, 2019.

[40] M. Thirumeni and D. Thangavelusamy, "Design and analysis of hybrid PSO-GSA tuned PI and SMC controller for DC-DC Cuk converter," *IET Circuits, Devices and Systems*, vol. 13, pp. 374–384, 2019.

[41] V. Bist and B. Singh, "A unity power factor bridgeless isolated Cuk converter-fed brushless DC motor drive," *IEEE Transactions on Industrial Electronics*, vol. 62, pp. 4118–4129, 2015.

[42] G. Marimuthu and M. G. Umamaheswari, "Analysis and design of single stage bridgeless Cuk converter for current harmonics suppression using particle swarm optimization technique," *Electric Power Components and Systems*, vol. 47, 2019.

[43] J. Gallardo-Lozano, E. Romero-Cadaval, M. I. Milanes-Montero, and M. A. Guerrero-Martinez, "Battery equalization active methods," *Journal of Power Sources*, vol. 246, pp. 934–949, 2014.

[44] C. Zhang, Y. Shang, Z. Li, and N. Cui, "An interleaved equalization architecture with self-learning fuzzy logic control for series-connected battery strings," *IEEE Transactions on Vehicular Technology*, vol. 66, pp. 10923–10934, 2017.

[45] Y. Yu, R. Saasaa, A. A. Khan, and W. Eberle, "A series resonant energy storage cell voltage balancing circuit," *IEEE Journal of Emerging and Selected Topics in Power Electronics*, vol. 8, pp. 3151–3161, 2020.

[46] M. Uno and A. Kukita, "Bidirectional PWM converter integrating cell voltage equalizer using series-resonant voltage multiplier for series-connected energy storage cells," *IEEE Transactions on Power Electronics*, vol. 30, pp. 3077–3090, 2015.

[47] X. Luo, L. Kang, C. Lu, J. Linghu, H. Lin, and B. Hu, "An enhanced multicell-to-multicell battery equalizer based on bipolar-resonant LC converter," *Electronics*, vol. 10, p. 293, 2021.

[48] V.-L. Pham, V. T. Duong, and W. Choi, "High-efficiency active cell-to-cell balancing circuit for Lithium-Ion battery modules using LLC resonant converter," *Journal of Power Electronics*, vol. 20, pp. 1037–1046, 2020.

[49] G. Farahani, "DC-DC series-resonant converter with multi stage current driven for balance charger of series connected lithium ion batteries," *IET Power Electronics*, vol. 14, pp. 992–1007, 2021.

[50] A. Sallam, A. A. Sopieh, and E. Nabil, "Battery management system performance enhancement using charge equalization controller design," *Menoufia Journal of Electronic Engineering Research*, vol. 2, pp. 55–63, 2022.

[51] U. K. Das, P. Shrivastava, K. S. Tey et al., "Advancement of lithium-ion battery cells voltage equalization techniques: a review," *Renewable and Sustainable Energy Reviews*, vol. 134, Article ID 110227, 2020.

[52] T. Gottwald, Z. Ye, and T. Stuart, "Equalization of EV and HEV batteries with a ramp converter," *IEEE Transactions on Aerospace and Electronic Systems*, vol. 33, pp. 307–312, 1997.

[53] M. K. Hasan, A. A. Habib, S. Islam, A. T. A. Ghani, and E. Hossain, "Resonant energy carrier base active charge-balancing algorithm," *Electronics*, vol. 9, p. 2166, 2020.

[54] D. Angulo-García, F. Angulo, and J. G. Muñoz, "DC-DC zeta power converter: ramp compensation control design and stability analysis," *Applied Sciences*, vol. 11, p. 5946, 2021.

[55] L. Zhao, D. J. Thrimawithana, U. K. Madawala, and A. P. Hu, "A push-pull parallel resonant converter-based bidirectional IPT system," *IEEE Transactions on Power Electronics*, vol. 35, pp. 2659–2667, 2020.

[56] J.-W. Lim, J. Hassan, and M. Kim, "Bidirectional soft switching push-pull resonant converter over wide range of battery voltages," *IEEE Transactions on Power Electronics*, vol. 36, pp. 12251–12267, 2021.

[57] V.-L. Pham, V. T. Duong, and W. Choi, "A low cost and fast cell-to-cell balancing circuit for lithium-Ion battery strings," *Electronics*, vol. 9, p. 248, 2020.

[58] K. R. Sree and A. K. Rathore, "Impulse commutated zero-current switching current-fed push-pull converter: analysis, design, and experimental results," *IEEE Transactions on Industrial Electronics*, vol. 62, pp. 363–370, 2015.

[59] J. Lu, Y. Wang, and X. Li, "Isolated bidirectional DC–DC converter with quasi-resonant zero-voltage switching for battery charge equalization," *IEEE Transactions on Power Electronics*, vol. 34, pp. 4388–4406, 2019.

[60] L. Li, Z. Huang, H. Li, and H. Lu, "A high-efficiency voltage equalization scheme for supercapacitor energy storage system in renewable generation applications," *Sustainability*, vol. 8, p. 548, 2016.

[61] V. Karthikeyan and R. Gupta, "Light-load efficiency improvement by extending ZVS range in DAB-bidirectional DC-DC converter for energy storage applications," *Energy*, vol. 130, pp. 15–21, 2017.

[62] X. Yu, X. She, X. Zhou, and A. Q. Huang, "Power management for DC microgrid enabled by solid-state transformer," *IEEE Transactions on Smart Grid*, vol. 5, pp. 954–965, 2014.

[63] A. K. Bhattacharjee and I. Batarseh, "Optimum hybrid modulation for improvement of efficiency over wide operating range for triple-phase-shift dual-active-bridge converter," *IEEE Transactions on Power Electronics*, vol. 35, pp. 4804–4818, 2020.

[64] S. S. Williamson, A. K. Rathore, and F. Musavi, "Industrial electronics for electric transportation: current state-of-the-art and future challenges," *IEEE Transactions on Industrial Electronics*, vol. 62, pp. 3021–3032, 2015.

[65] Y. Shang, B. Xia, C. Zhang, N. Cui, J. Yang, and C. C. Mi, "An automatic equalizer based on forward-flyback converter for series-connected battery strings," *IEEE Transactions on Industrial Electronics*, vol. 64, pp. 5380–5391, 2017.

[66] G. Xiangwei, G. Jiahao, L. Zhen, L. Kang, and X. Xiaozhuo, "Active balancing method for series battery pack based on

flyback converter," *IET Circuits, Devices and Systems*, vol. 14, pp. 1129–1134, 2020.

[67] V. Cardoso, S. L. Brockveld Junior, T. B. Lazzarin, and G. Waltrich, "Double boost-flyback converter," *IET Power Electronics*, vol. 13, pp. 1163–1171, 2020.

[68] J. Cao, B. Xia, and J. Zhou, "An active equalization method for lithium-ion batteries based on flyback transformer and variable step size generalized predictive control," *Energies*, vol. 14, p. 207, 2021.

[69] H. Xiong, D. Song, F. Shi, Y. Wei, and L. Jinzhen, "Novel voltage equalisation circuit of the lithium battery pack based on bidirectional flyback converter," *IET Power Electronics*, vol. 13, pp. 2194–2200, 2020.

[70] Y.-C. Hsieh, L.-R. Yu, and M.-F. Yang, "A charge equalization scheme for battery string with charging current allocation," *International Journal of Circuit Theory and Applications*, vol. 49, pp. 2935–2945, 2021.

[71] Y. Cao, K. Li, and M. Lu, "Balancing method based on flyback converter for series-connected cells," *IEEE Access*, vol. 9, pp. 52393–52403, 2021.

[72] F. Shi and D. Song, "A novel high-efficiency double-input bidirectional DC/DC converter for battery cell-voltage equalizer with flyback transformer," *Electronics*, vol. 8, p. 1426, 2019.

[73] Y.-L. Lee, C.-H. Lin, and S.-J. Yang, "Power loss analysis and a control strategy of an active cell balancing system based on a bidirectional flyback converter," *Applied Sciences*, vol. 10, p. 4380, 2020.

[74] Y. Shang, B. Xia, C. Zhang, N. Cui, J. Yang, and C. Mi, "A modularization method for battery equalizers using multiwinding transformers," *IEEE Transactions on Vehicular Technology*, vol. 66, pp. 8710–8722, 2017.

[75] H. A. Gabbar, A. M. Othman, and M. R. Abdussami, "Review of battery management systems (BMS) development and industrial standards," *Technologies*, vol. 9, p. 28, 2021.

[76] C. Zhang, Y. Li, J. Huang, Z. Xia, and J. Liu, "Research on alternating equalization control systems for lithium-ion cells charging," *World Electric Vehicle Journal*, vol. 12, 2021.

[77] A. Tavakoli, S. A. Khajehoddin, and J. Salmon, "Control and analysis of a modular bridge for battery cell voltage balancing," *IEEE Transactions on Power Electronics*, vol. 33, pp. 9722–9733, 2018.

[78] F. Feng, X. Hu, J. Liu, X. Lin, and B. Liu, "A review of equalization strategies for series battery packs: variables, objectives, and algorithms," *Renewable and Sustainable Energy Reviews*, vol. 116, Article ID 109464, 2019.

[79] L. Song, K. Zhang, T. Liang, X. Han, and Y. Zhang, "Intelligent state of health estimation for lithium-ion battery pack based on big data analysis," *Journal of Energy Storage*, vol. 32, Article ID 101836, 2020.

[80] M. Einhorn, W. Roessler, and J. Fleig, "Improved performance of serially connected Li-ion batteries with active cell balancing in electric vehicles," *IEEE Transactions on Vehicular Technology*, vol. 60, no. 6, pp. 2448–2457, 2011.

[81] C. Zhang, Y. Jiang, J. Jiang, G. Cheng, W. Diao, and W. Zhang, "Study on battery pack consistency evolutions and equilibrium diagnosis for serial-connected lithium-ion batteries," *Applied Energy*, vol. 207, pp. 510–519, 2017.

[82] Y. Zheng, L. Lu, X. Han, J. Li, and M. Ouyang, "$LiFePO_4$ battery pack capacity estimation for electric vehicles based on charging cell voltage curve transformation," *Journal of Power Sources*, vol. 226, pp. 33–41, 2013.

[83] A. Wadi, M. Abdel-Hafez, A. Hussein, and F. Alkhawaja, "Alleviating dynamic model uncertainty effects for improved battery SOC estimation of EVs in highly dynamic environments," *IEEE Transactions on Vehicular Technology*, vol. 70, no. 7, pp. 6554–6566, 2021.

[84] A. Samanta and S. Chowdhuri, "Active cell balancing of lithium-ion battery pack using dual DC-DC converter and auxiliary lead-acid battery," *Journal of Energy Storage*, vol. 33, Article ID 102109, 2021.

[85] Q. Ouyang, W. Han, C. Zou, G. Xu, and Z. Wang, "Cell balancing control for lithium-ion battery packs: a hierarchical optimal approach," *IEEE Transactions on Industrial Informatics*, vol. 16, pp. 5065–5075, 2020.

[86] M. Uzair, G. Abbas, and S. Hosain, "Characteristics of battery management systems of electric vehicles with consideration of the active and passive cell balancing process," *World Electric Vehicle Journal*, vol. 12, p. 120, 2021.

[87] F. Naseri, E. Schaltz, D. I. Stroe, A. Gismero, and E. Farjah, "An enhanced equivalent circuit model with real-time parameter identification for battery state-of-charge estimation," *IEEE Transactions on Industrial Electronics*, vol. 69, pp. 3743–3751, 2022.

[88] C. N. Van, T. N. Vinh, M. D. Ngo, and S. J. Ahn, "Optimal SoC balancing control for lithium-ion battery cells connected in series," *Energies*, vol. 14, no. 10, p. 2875, 2021.

[89] W. Han, C. Zou, C. Zhou, and L. Zhang, "Estimation of cell SOC evolution and system performance in module-based battery charge equalization systems," *IEEE Transactions on Smart Grid*, vol. 10, pp. 4717–4728, 2019.

[90] X. Liu, Y. Sun, Y. He, X. Zheng, G. Zeng, and J. Zhang, "Battery equalization by fly-back transformers with inductance, capacitance and diode absorbing circuits," *Energies*, vol. 10, p. 1482, 2017.

[91] M. A. Hannan, D. N. T. How, M. S. H. Lipu et al., "SOC estimation of li-ion batteries with learning rate-optimized deep fully convolutional network," *IEEE Transactions on Power Electronics*, vol. 36, pp. 7349–7353, 2021.

[92] X. Tang, Y. Wang, and Z. Chen, "A method for state-of-charge estimation of $LiFePO_4$ batteries based on a dual-circuit state observer," *Journal of Power Sources*, vol. 296, pp. 23–29, 2015.

[93] C. Truchot, M. Dubarry, and B. Y. Liaw, "State-of-charge estimation and uncertainty for lithium-ion battery strings," *Applied Energy*, vol. 119, pp. 218–227, 2014.

[94] B. Balasingam, M. Ahmed, and K. Pattipati, "Battery management systems—challenges and some solutions," *Energies*, vol. 13, p. 2825, 2020.

[95] T. Girijaprasanna and C. Dhanamjayulu, "A review on different state of battery charge estimation techniques and management systems for EV applications," *Electronics*, vol. 11, 2022.

[96] J. Rivera-Barrera, N. Muñoz-Galeano, and H. Sarmiento-Maldonado, "SoC estimation for lithium-ion batteries: review and future challenges," *Electronics*, vol. 6, 2017.

[97] T.-H. Wu and C. S. Moo, "State-of-charge estimation with state-of-health calibration for lithium-ion batteries," *Energies*, vol. 10, p. 987, 2017.

[98] J. Chen, Q. Ouyang, C. Xu, and H. Su, "Neural network-based state of charge observer design for lithium-ion batteries," *IEEE Transactions on Control Systems Technology*, vol. 26, pp. 313–320, 2018.

[99] X. Tang, F. Gao, K. Liu, Q. Liu, and A. M. Foley, "A balancing current ratio-based state-of-health estimation solution for lithium-ion battery pack," *IEEE Transactions on Industrial Electronics*, vol. 69, pp. 8055–8065, 2022.

[100] F. Yang, W. Li, C. Li, and Q. Miao, "State-of-charge estimation of lithium-ion batteries based on gated recurrent neural network," *Energy*, vol. 175, pp. 66–75, 2019.

[101] P. Shrivastava, T. K. Soon, M. Y. I. B. Idris, and S. Mekhilef, "Overview of model-based online state-of-charge estimation using Kalman filter family for lithium-ion batteries," *Renewable and Sustainable Energy Reviews*, vol. 113, Article ID 109233, 2019.

[102] A. Gismero, I. S. Daniel, and E. Schaltz, "Comparative study of state of charge estimation under different open circuit voltage test conditions for lithium-ion batteries," in *Proceedings of the IECON 2020 the 46th Annual Conference of the IEEE Industrial Electronics Society*, Singapore, October 2020.

[103] T. Wu, F. Ji, L. Liao, and C. Chang, "Voltage-SOC balancing control scheme for series-connected lithium-ion battery packs," *Journal of Energy Storage*, vol. 25, Article ID 100895, 2019.

[104] Z. Xia and J. A. Abu Qahouq, "State-of-charge balancing of lithium-ion batteries with state-of-health awareness capability," *IEEE Transactions on Industry Applications*, vol. 57, pp. 673–684, 2021.

[105] M. Zhang and X. Fan, "Review on the state of charge estimation methods for electric vehicle battery," *World Electric Vehicle Journal*, vol. 11, 2020.

[106] J. Meng, M. Ricco, G. Luo et al., "An overview and comparison of online implementable SOC estimation methods for lithium-ion battery," *IEEE Transactions on Industry Applications*, vol. 54, no. 2, pp. 1583–1591, 2018.

[107] S. Wang, S. Yang, W. Yang, and Y. Wang, "A new kind of balancing circuit with multiple equalization modes for serially connected battery pack," *IEEE Transactions on Industrial Electronics*, vol. 68, 2020.

[108] M.-Y. Kim, W. K. Jong, C. H. Kim, S. Y. Cho, G. W. Moon, and W. K. Jong, "Automatic charge equalization circuit based on regulated voltage source for series connected lithium-ion batteries," in *Proceedings of the 8th International Conference on Power Electronics-ECCE Asia*, Jeju, Republic of Korea, May 2011.

[109] M. M. Hoque, M. Hannan, A. Mohamed, and A. Ayob, "Battery charge equalization controller in electric vehicle applications: a review," *Renewable and Sustainable Energy Reviews*, vol. 75, pp. 1363–1385, 2017.

[110] I.-O. Lee, "Hybrid PWM-resonant converter for electric vehicle on-board battery chargers," *IEEE Transactions on Power Electronics*, vol. 31, pp. 3639–3649, 2016.

[111] J. Sun, C. Zhu, R. Lu, K. Song, and G. Wei, "Development of an optimized algorithm for bidirectional equalization in lithium-ion batteries," *Journal of Power Electronics*, vol. 15, pp. 775–785, 2015.

[112] N. Hou, W. Song, Y. Li, Y. Zhu, and Y. Zhu, "A comprehensive optimization control of dual-active-bridge DC–DC converters based on unified-phase-shift and power-balancing scheme," *IEEE Transactions on Power Electronics*, vol. 34, pp. 826–839, 2019.

[113] X. Guo, J. Geng, Z. Liu, X. Xu, and W. Cao, "A flyback converter-based hybrid balancing method for series-connected battery pack in electric vehicles," *IEEE Transactions on Vehicular Technology*, vol. 70, pp. 6626–6635, 2021.